Check for updates

ORIGINAL ARTICLE

# Plasma Metabolomics Reveals Distinct Biological and Diagnostic Signatures for Melioidosis

Lu Xia[1], Viriya Hantrakun[5], Prapit Teparrukkul[8], Gumphol Wongsuvan[5], Taniya Kaewarpai[6], Adul Dulsuk[6], Nicholas P. J. Day[5,9], Rozenn N. Lemaitre[2], Narisara Chantratita[5,6], Direk Limmathurotsakul[5,7]*, Ali Shojaie[1]*, Sina A. Gharib[3]*, and T. Eoin West[3,4]*

[1]Department of Biostatistics, [2]Cardiovascular Health Research Unit and [3]Division of Pulmonary, Critical Care, and Sleep Medicine, Department of Medicine, and [4]Department of Global Health, University of Washington, Seattle, Washington; [5]Mahidol Oxford Tropical Medicine Research Unit, [6]Department of Microbiology and Immunology, and [7]Department of Tropical Hygiene, Faculty of Tropical Medicine, Mahidol University, Bangkok, Thailand; [8]Department of Internal Medicine, Sunpasitthiprasong Hospital, Ubon Ratchathani, Thailand; and [9]Centre for Tropical Medicine and Global Health, Nuffield Department of Medicine, University of Oxford, Oxford, United Kingdom

ORCID IDs: 0000-0003-1561-6871 (L.X.); 0000-0002-6727-3404 (V.H.); 0000-0003-2309-1171 (N.P.J.D.); 0000-0002-7038-1844 (R.N.L.); 0000-0001-7240-5320 (D.L.); 0000-0001-8846-3533 (A.S.); 0000-0002-2480-4367 (S.A.G.); 0000-0001-5503-7204 (T.E.W.).

## Abstract

**Rationale:** The global burden of sepsis is greatest in low-resource settings. Melioidosis, infection with the gram-negative bacterium *Burkholderia pseudomallei*, is a frequent cause of fatal sepsis in endemic tropical regions such as Southeast Asia.

**Objectives:** To investigate whether plasma metabolomics would identify biological pathways specific to melioidosis and yield clinically meaningful biomarkers.

**Methods:** Using a comprehensive approach, differential enrichment of plasma metabolites and pathways was systematically evaluated in individuals selected from a prospective cohort of patients hospitalized in rural Thailand with infection. Statistical and bioinformatics methods were used to distinguish metabolomic features and processes specific to patients with melioidosis and between fatal and nonfatal cases.

**Measurements and Main Results:** Metabolomic profiling and pathway enrichment analysis of plasma samples from patients with melioidosis ($n = 175$) and nonmelioidosis infections ($n = 75$) revealed a distinct immuno-metabolic state among patients with melioidosis, as suggested by excessive tryptophan catabolism in the kynurenine pathway and significantly increased levels of sphingomyelins and ceramide species. We derived a 12-metabolite classifier to distinguish melioidosis from other infections, yielding an area under the receiver operating characteristic curve of 0.87 in a second validation set of patients. Melioidosis nonsurvivors ($n = 94$) had a significantly disturbed metabolome compared with survivors ($n = 81$), with increased leucine, isoleucine, and valine metabolism, and elevated circulating free fatty acids and acylcarnitines. A limited eight-metabolite panel showed promise as an early prognosticator of mortality in melioidosis.

**Conclusions:** Melioidosis induces a distinct metabolomic state that can be examined to distinguish underlying pathophysiological mechanisms associated with death. A 12-metabolite signature accurately differentiates melioidosis from other infections and may have diagnostic applications.

**Keywords:** *Burkholderia pseudomallei* infection; immune responses; metabolic pathways; predictive modeling; sepsis

(Received in original form July 18, 2022; accepted in final form October 9, 2023)

This article is open access and distributed under the terms of the Creative Commons Attribution Non-Commercial No Derivatives License 4.0. For commercial usage and reprints, please e-mail Diane Gern (dgern@thoracic.org).

*Co–senior authors.

Supported by NIH grants R01HL113382, R01AI137111, R01GM114029, and R21AI173435; and the Wellcome Trust grants 090219/Z/09/Z and 101103/Z/13/Z. The funders had no role in study design, data collection and analysis, decision to publish, or preparation of the manuscript.

Author Contributions: L.X., N.P.J.D., N.C., D.L., A.S., S.A.G., and T.E.W. participated in the study design and the conception of this work. V.H., P.T., G.W., T.K., A.D., N.C., and D.L. contributed to the acquisition of the data, and N.C., V.H., and D.L. verified the data. L.X. led the data analysis and wrote the first draft of the manuscript. R.N.L., D.L., A.S., S.A.G., and T.E.W. contributed to interpreting the data and editing the manuscript. All authors have read and approved the manuscript before submission.

Data sharing statement: Deidentified demographic information and metabolomic data have been deposited in Metabolomics Workbench (Study ID: ST002909) and can be accessed at https://dx.doi.org/10.21228/M8W71R.

Am J Respir Crit Care Med Vol 209, Iss 3, pp 288–298, Feb 1, 2024
Copyright © 2024 by the American Thoracic Society
Originally Published in Press as DOI: 10.1164/rccm.202207-1349OC on October 9, 2023
Internet address: www.atsjournals.org

## At a Glance Commentary

**Scientific Knowledge on the Subject:** Melioidosis is an infectious disease endemic in Southeast Asia with high mortality despite administration of antimicrobial treatments. The metabolomic signals induced by this infection are poorly understood but may provide insights into its pathogenesis and yield diagnostic and prognostic biomarkers.

**What This Study Adds to the Field:** This study is the most comprehensive metabolomic assessment of melioidosis to date. We found that melioidosis induces a distinct metabolic state that can be probed to discern its underlying pathophysiological mechanisms. Metabolic signatures were derived and confirmed to accurately differentiate melioidosis from other infections and may help predict risk of death.

The global burden of sepsis approaches 50 million cases annually and is most impactful in low-resource settings (1). Reducing this health burden requires research in diverse at-risk populations because of global heterogeneity in host factors, etiologic pathogens, and clinical capacity (2). For example, in tropical regions such as Southeast Asia and northern Australia, melioidosis, an infection caused by the gram-negative bacterium *Burkholderia pseudomallei*, is a common cause of severe infection and sepsis (3). Melioidosis can be acquired through ingestion, inhalation, or percutaneous inoculation of *B. pseudomallei*, an environmental saprophyte. Melioidosis is considered to be an emerging global threat in many countries, including the United States: in 2022, the CDC isolated *B. pseudomallei* from soil and water samples in the Gulf Coast region of Mississippi after two unrelated cases of melioidosis infection were reported in this area, indicating that this infection is now autochthonous in the continental United States (4). Melioidosis is likely underreported throughout the tropics, but in Southeast Asia case fatality rates of confirmed infections reach 50% (3). To improve outcomes from this emerging infection, a better understanding of melioidosis pathogenesis and development of novel diagnostic and predictive biomarkers are urgently needed.

Metabolomics systematically studies small molecules as products of metabolism and can be used to investigate responses to host–pathogen interactions, disease states, nutritional changes, and stress (5). Hence, metabolomics has been used as an informative tool for improving diagnosis and prognosis of sepsis (6–8). However, there have been few studies of metabolomics in human melioidosis. We hypothesized that infection with *B. pseudomallei* induces distinctive metabolomic perturbations in plasma that reflect dysregulated pathways, and that this information can be exploited to distinguish melioidosis from other infections and to predict clinically meaningful outcomes in melioidosis. In this study, we leveraged one of the only large prospective studies of patients with severe infection and sepsis in rural northeastern Thailand to conduct large-scale plasma metabolomics analyses, with the aims of identifying differentially altered metabolites and pathways in melioidosis. We leveraged this information to build diagnostic and prognostic molecular classifiers. This investigation reflects the potential power of applying omics technologies to severe infection and sepsis in low-resource settings to improve knowledge about pathophysiologic mechanisms attributable to priority pathogens and to develop diagnostic and prognostic tools.

## Methods

### Study Design, Participants, and Clinical Data

Subjects at least 18 years of age admitted to Sunpasitthiprasong Hospital in Ubon Ratchathani, Thailand with suspected community-acquired infection were sequentially and prospectively enrolled within 24 hours of admission into the Ubon-Sepsis parent study from 2013 through 2017. This cohort has been described previously (9–15). Plasma samples were obtained from all participants at the time of enrollment. For the current analysis, plasma from a random sampling of all patients with melioidosis (as determined by a positive culture for *B. pseudomallei* from any clinical sample) and plasma from random samplings of patients with *Escherichia coli*, *Staphylococcus aureus*, or *Klebsiella pneumoniae* bacteremias (the most common) and a set of patients who had suspected infection but negative blood cultures and no positive culture for *B. pseudomallei* were selected from the parent study. Further details about the diagnosis of infection are provided in the online supplement. Plasma was also analyzed from random samplings of nonhospitalized control individuals (without active infections) with either diabetes or no relevant medical conditions who were recruited from the outpatient clinic and blood donation center at Udon Thani Hospital, Udon Thani, Thailand. Control subjects with diabetes were included because diabetes is a major risk factor for acquisition of melioidosis (3). Random samplings were performed using the Stata function runiform. These hospitalized, infected patients and the outpatient control subjects together were designated as cohort 1. With limited studies having a similar design to ours, plasma from a second independent set of patients from the same parent study were analyzed separately for validation (cohort 2). The following demographic and clinical variables were considered: age (yr), sex, body mass index (BMI), modified Sequential Organ Failure Assessment (SOFA) score (10, 16) (*see* the online supplement), 28-day mortality, and histories of diabetes, chronic kidney, heart, liver, and lung diseases, hypertension, dyslipidemia, stroke, and cancer, all of which were coded as binary indicators.

### Metabolomics Analysis

Sample preparation and ultrahigh-performance liquid chromatography–tandem mass spectroscopy analyses were

Correspondence and requests for reprints should be addressed to Sina A. Gharib, M.D., Center for Lung Biology, 850 Republican Street, Seattle, WA 98109. E-mail: sagharib@uw.edu.

This article has a related editorial.

This article has an online supplement, which is accessible from this issue's table of contents at www.atsjournals.org.

performed by Metabolon, Inc., as described in the online supplement.

### Statistical Analysis

Data were analyzed in R statistical environment (R Core Team, 2022). Metabolites with >25% missing values in each infection group in cohort 1 were excluded from further analysis. The relative abundance measure for metabolites was $\log_2$-transformed. The missing values in the remaining metabolites were imputed according to the procedure described in the online supplement.

Uniform Manifold Approximation and Projection (UMAP) was used to visualize the clustering of samples (R package umap, version 0.2.8.0) (17). We conducted unadjusted analysis via two-sided Welch's *t* test and analysis adjusted for covariates (i.e., age, sex, BMI, and diabetes when comparing melioidosis with other etiologies; age, sex, BMI, and chronic kidney disease in analyses of 28-day mortality among patients with melioidosis) via linear regression to identify differential metabolites. The global test, a functional class scoring method that tests for differential pathways, was used for pathway analysis with R package globaltest (version 5.50.0) (18). For differential metabolite and pathway enrichment analyses, adjusted *P* values were obtained using the conservative Holm's procedure for family-wise error rate control, and significance was determined at <0.05.

To identify diagnostic metabolites for melioidosis and prognostic metabolites for 28-day mortality in patients with melioidosis, regularized logistic regression with Lasso penalty was used with R package glmnet (version 4.1.4) (19). To ensure consistency, we restricted diagnostic and prognostic modeling to nondrug metabolites that had <5% overall missingness in both cohort 1 and cohort 2. Within cohort 1, 80% of target populations (all hospitalized patients for diagnostic biomarker analysis or all patients with melioidosis for prognostic biomarker analysis) were randomly withheld for biomarker discovery and the remaining 20% for validation (validation 1). Repeated sample splitting of the discovery data was performed as described in the online supplement. Metabolites were ranked by their average selection frequency and coefficient estimates using Lasso, and top metabolites were carried into logistic regression models for assessing different numbers of diagnostic or prognostic metabolites in the validation 1 set and for separate validation in cohort 2.

### Human Subjects

This study was approved by the Mahidol University Faculty of Tropical Medicine Ethics Committee (MUTM 2012-024-01 and MUTM 2018-046-01), the Sunpasitthiprasong Hospital Ethics Committee (039/2556), the Udon Thani Hospital Ethics Committee, the University of Washington Institutional Review Board (42988), and the University of Oxford Tropical Research Ethics Committee (OXTREC172-12). Informed consent was obtained from all study participants or their representatives.

## Results

### Subject Recruitment and Characteristics

Cohort 1 comprised 300 individuals recruited in rural northeastern Thailand: 250 patients who were hospitalized with suspected community-acquired infection enrolled into the Ubon-Sepsis study and 50 nonhospitalized adults as uninfected control subjects ($n = 25$ healthy and $n = 25$ subjects with diabetes). For hospitalized patients with infection, plasma samples were drawn within 24 hours of admission; the etiologies of infection were as follows: $n = 175$ with *B. pseudomallei* (from any culture), $n = 22$ with *E. coli* bacteremia, $n = 16$ with *S. aureus* bacteremia, $n = 15$ with *K. pneumoniae* bacteremia, and $n = 22$ patients with negative blood cultures and no culture positive for *B. pseudomallei*. Demographic, clinical, and outcome variables are summarized in Table 1. Compared with other infections, patients with melioidosis were on average younger, more likely to be male, and more likely to have diabetes (*P* value = 0.005, 0.02, and 0.001, respectively; *see* Table E1 in the

**Table 1.** Demographics and Clinical Variables of Cohort 1 Study Population

| Variable | Uninfected Control Subjects | Melioidosis | *E. coli* | *S. aureus* | *K. pneumoniae* | Culture-Negative |
|---|---|---|---|---|---|---|
| *N* | 50 | 175 | 22 | 16 | 15 | 22 |
| Age, yr, median (IQR) | 50.5 (18.3) | 54.0 (18.5) | 67.0 (14.8) | 61.5 (22.3) | 64.0 (31.5) | 59.0 (23.3) |
| Female | 20 (40) | 54 (31) | 11 (50) | 4 (25) | 8 (53) | 12 (55) |
| BMI, median (IQR) | 24.4 (4.9) | 21.9 (4.3) | 21.8 (3.3) | 22.9 (6.5) | 21.5 (4.8) | 21.6 (4.4) |
| Modified SOFA score, median (IQR) | — | 5.0 (7.0) | 5.0 (6.8) | 4.0 (8.5) | 4.0 (4.0) | 4.0 (2.8) |
| Diabetes | 25 (50) | 84 (48) | 4 (18) | 7 (44) | 4 (27) | 4 (18) |
| Hypertension | — | 43 (25) | 6 (27) | 6 (38) | 2 (13) | 6 (27) |
| Chronic kidney disease | — | 26 (15) | 4 (18) | 4 (25) | 2 (13) | 5 (23) |
| Chronic heart disease | — | 8 (5) | 4 (18) | 0 | 1 (7) | 0 |
| Chronic liver disease | — | 6 (3) | 2 (9) | 1 (6) | 0 | 1 (5) |
| Chronic lung disease | — | 13 (7) | 0 | 0 | 2 (13) | 1 (5) |
| Dyslipidemia | — | 10 (6) | 2 (9) | 1 (6) | 1 (7) | 0 |
| Stroke | — | 2 (1) | 2 (9) | 0 | 1 (7) | 0 |
| Cancer | — | 3 (2) | 0 | 0 | 0 | 1 (5) |
| Death by Day 28 | — | 94 (54) | 5 (23) | 5 (31) | 5 (33) | 4 (18) |

*Definition of abbreviations*: BMI = body mass index; *E. coli* = *Escherichia coli*; IQR = interquartile range; *K. pneumoniae* = *Klebsiella pneumoniae*; *S. aureus* = *Staphylococcus aureus*; SOFA = Sequential Organ Failure Assessment.
Data represent count (percentage) within each group, unless otherwise noted.

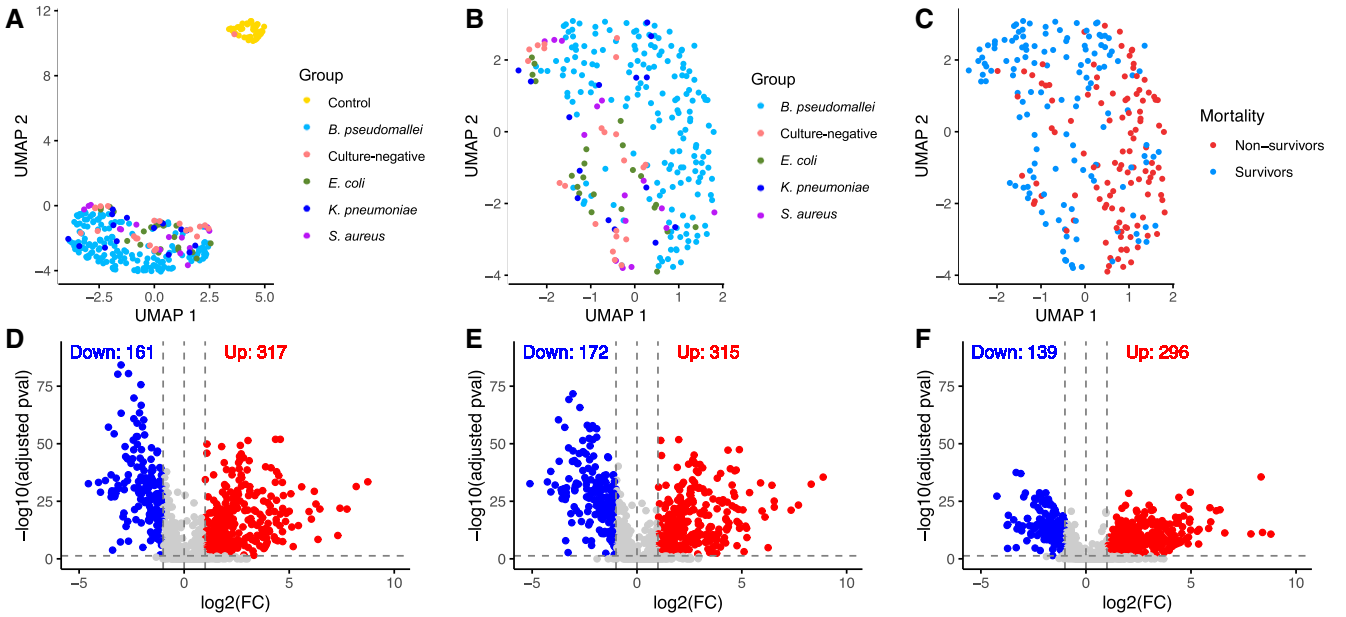


**Figure 1.** UMAP visualization of the metabolome of (*A*) all 300 subjects in cohort 1; (*B*) 250 patients hospitalized with infection, labeled by infection group; and (*C*) 250 patients hospitalized with infection, labeled by 28-day mortality. Volcano plots comparing (*D*) all hospitalized patients with the uninfected control subjects; (*E*) patients with melioidosis with the uninfected control subjects; and (*F*) patients with infections other than melioidosis with the uninfected control subjects. Significant metabolites with greater than two-fold change are highlighted; red: increased abundance, blue: decreased abundance. *B. pseudomallei* = *Burkholderia pseudomallei*; *E. coli* = *Escherichia coli*; FC = fold change; *K. pneumoniae* = *Klebsiella pneumoniae*; *S. aureus* = *Staphylococcus aureus*; UMAP = Uniform Manifold Approximation and Projection.

online supplement). A higher proportion of patients with melioidosis died by 28 days after hospital admission (94 out of 175, 54%) than of those with other etiologies (19 out of 75, 25%) ($P$ value = $4.9 \times 10^{-5}$). Modified SOFA score and chronic kidney disease were significantly associated with 28-day mortality among patients with melioidosis ($P$ value = $3.0 \times 10^{-12}$ and 0.03, respectively; Table E2).

### Metabolomic Profiling of Subject Groups

In cohort 1, 1,448 metabolites were measured in the plasma samples, and >80% of the metabolites (1,181) were chemically identified and were included for subsequent analyses. After exclusion of 112 drug metabolites and 119 identified metabolites with >25% missing values in each subject group, 950 identified metabolites remained for final analyses.

We compared the plasma metabolomes of patients with melioidosis, patients hospitalized with other infections, and uninfected control subjects in cohort 1. Dimension reduction using UMAP demonstrated striking differences between hospitalized patients with infection and uninfected control subjects (Figure 1A) and the separation of patients with melioidosis from patients with other infections (Figure 1B). One patient in the culture-negative group clustered with the uninfected control subjects and was excluded from further analysis (Figure 1A; *see* the online supplement for details). For patients hospitalized with infection, we evaluated the UMAP plot stratified by 28-day mortality (Figure 1C), as well as by age, modified SOFA score, BMI, sex, and diabetes (Figures E1A–E1E), and observed evident patterns for mortality and modified SOFA score.

### Hospitalized Patients with Infection Have Profound Metabolomic Changes

In unadjusted univariate analyses, 706 metabolites were differentially altered between hospitalized patients and the uninfected control subjects (Figure 1D and Table E3A). The differentially abundant metabolites reflected a highly activated inflammatory or immune state among the hospitalized patients. We then separately compared the metabolomes of patients with melioidosis or those with other infections to the uninfected control subjects, resulting in 691 and 607 significant metabolites, respectively (Figures 1E and 1F and Tables E3B and E3C), and found that 569 differentially abundant metabolites overlapped between the two comparisons (Figure E2). This observation implies that severe infection, regardless of etiology, results in disturbance to many shared metabolic pathways but that there are also differentially abundant metabolites unique to melioidosis.

### A Diverse Set of Metabolites Distinguish Melioidosis from Other Infections

We next investigated whether melioidosis is associated with a distinct metabolomic signature compared with other infections. After adjusting for age, sex, BMI, and diabetes, we identified 75 significantly differentially abundant metabolites between patients with melioidosis and those with other infections (Figure 2A and Table E3D). Other preexisting comorbidities were not found to be associated with melioidosis (Table E1) and, thus, were not included in the model. Although diabetes is a major risk factor for melioidosis (3), no significant evidence suggested that diabetes modified

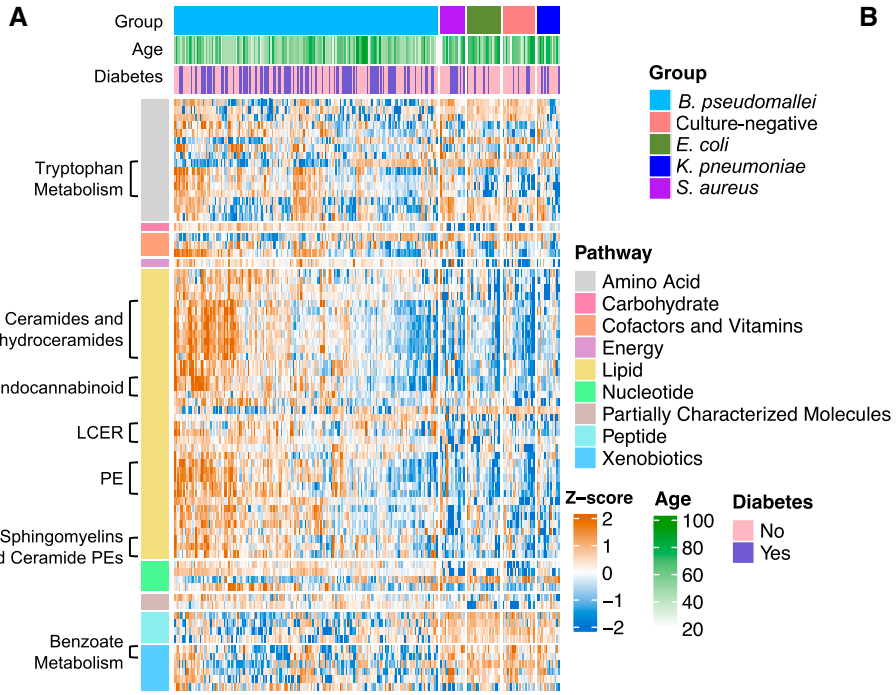


**Figure 2.** (*A*) Heatmap of 75 significantly differentially abundant metabolites between patients with melioidosis and patients with other infections, adjusted for age, sex, body mass index, and diabetes. (*B*) Boxplots of eight representative metabolites from various pathways comparing levels in patients with melioidosis to levels in patients with other infections. *P* values shown were calculated using Welch's *t* test. *B. pseudomallei* = *Burkholderia pseudomallei*; *E. coli* = *Escherichia coli*; *K. pneumoniae* = *Klebsiella pneumoniae*; LCER = lactosylceramides; PE = phosphatidylethanolamine; *S. aureus* = *Staphylococcus aureus*.

the associations between metabolite levels and infection groups after we examined the interactions.

Twenty-one pathways were differentially enriched among patients with melioidosis compared with patients with other suspected infections, after adjusting for age, sex, BMI, and diabetes (Table 2). These significant pathways spanned six superpathways: Amino Acid, Cofactors and Vitamins, Lipid, Nucleotide, Peptide, and Xenobiotics. The Tryptophan Metabolism pathway, within the Amino Acid superpathway, was significantly dysregulated in patients with melioidosis (Table 2 and Figure 2A). 3-hydroxykynurenine, kynurenine, and quinolinate in the Tryptophan Metabolism pathway were all in higher levels among patients with melioidosis (Figure 2B), and 6-bromotryptophan was reduced in the same group (Table E3D). When we included the modified SOFA score to account for severity of illness in our model, all previously identified 75 metabolites as well as 17 additional metabolites were found to be significantly differentially abundant in patients with melioidosis compared with patients with other infections (Table E4). Five of these 17 metabolites with modified SOFA adjustment belonged to the Tryptophan Metabolism pathway, suggesting that activation of the Tryptophan Metabolism pathway may be unique to melioidosis independent of severity of illness. The kynurenine-to-tryptophan ratio, an indicator of indoleamine 2,3-dioxygenase activity, was compared between patients with melioidosis and patients with other infections and showed a significant increase among patients with melioidosis (Figure E3A). We also observed that many altered metabolic pathways specific to patients with melioidosis were within the Lipid superpathway, including the highly enriched Ceramides and Dihydroceramides pathway, Phosphatidylethanolamines (PEs), Lactosylceramides, Endocannabinoid, and Sphingomyelins and Ceramide PEs (Table 2 and Figure 2A). For example, ceramide (d18:2/24:1, d18:1/24:2), sphingomyelin (d18:2/16:0, d18:1/16:1), and an endocannabinoid metabolite, palmitoyl ethanolamide, were all enriched in patients with melioidosis relative to other infections (Figure 2B). The Purine Metabolism pathway, within the Nucleotide superpathway, was also more abundant in patients with melioidosis (Table 2), including the most significantly abundant metabolite, adenosine (Figure 2B).

### Metabolomic Biomarkers Can Identify Melioidosis Cases Among Hospitalized Patients

Accurate and rapid diagnosis of the etiology of infection is critical to informing appropriate antimicrobial selection, triage, and referral decisions and mitigating the likelihood of poor outcomes, especially in resource-limited rural regions. Biomarkers in plasma obtained shortly after clinical presentation have the potential to fulfill this need. To develop and confirm a metabolomic biomarker panel for distinguishing melioidosis from other etiologies of infection, we generated discovery ($n = 200$) and validation ($n = 49$) sets in the hospitalized, infected patients within cohort 1 to build models and assess their performance (Figure 3A). Using the discovery set, repeated data splitting with Lasso that incorporated 519 metabolites generated a ranked list of metabolites by their

**Table 2.** Significantly Altered Pathways in Patients with Melioidosis Compared with Other Infections

| Superpathway | Pathway | Adjusted *P* Value | Total No. Metabolites |
|---|---|---|---|
| Amino Acid | Tryptophan Metabolism | $2.52 \times 10^{-7}$ | 26 |
| | Glutathione Metabolism | $1.71 \times 10^{-2}$ | 7 |
| Cofactors and Vitamins | Tocopherol Metabolism | $3.70 \times 10^{-3}$ | 3 |
| | Vitamin B2, B3, B5, and B6 Metabolism | $3.67 \times 10^{-2}$ | 12 |
| Lipid | Ceramides and Dihydroceramides | $8.90 \times 10^{-6}$ | 12 |
| | Endocannabinoid | $8.61 \times 10^{-5}$ | 9 |
| | Androgenic Steroids | $2.60 \times 10^{-4}$ | 22 |
| | Phosphatidylethanolamine | $7.04 \times 10^{-4}$ | 14 |
| | Lactosylceramides | $7.67 \times 10^{-4}$ | 5 |
| | Secondary Bile Acid Metabolism | $2.80 \times 10^{-3}$ | 21 |
| | Primary Bile Acid Metabolism | $7.03 \times 10^{-3}$ | 13 |
| | Phospholipid, Inositol and Glycerolipid Metabolism, and Phosphatidylserine | $2.12 \times 10^{-2}$ | 12 |
| | Fatty Acid Metabolism (Acyl Carnitine, Long-Chain Saturated) | $2.71 \times 10^{-2}$ | 9 |
| | Phosphatidylcholine | $2.76 \times 10^{-2}$ | 18 |
| | Diacylglycerol | $3.45 \times 10^{-2}$ | 31 |
| Nucleotide | Pyrimidine Metabolism | $4.33 \times 10^{-3}$ | 22 |
| | Purine Metabolism | $1.33 \times 10^{-2}$ | 15 |
| Peptide | Dipeptide | $1.24 \times 10^{-7}$ | 6 |
| | γ-glutamyl Amino Acid | $1.25 \times 10^{-2}$ | 17 |
| Xenobiotics | Benzoate Metabolism | $1.14 \times 10^{-3}$ | 22 |
| | Nutrition | $1.85 \times 10^{-3}$ | 43 |

Twenty-one significantly altered pathways in patients with melioidosis compared with other infections using the global test, adjusting for age, sex, body mass index, and diabetes, with Holm's adjusted *P* values and total numbers of metabolites in each pathway.

selection frequency (Figure 3B). After assessing the areas under the receiver operating characteristic curve (AUCs) of logistic regression models sequentially incorporating the top 1 to the top 15 metabolites (Figure E4A), a 12-metabolite signature (Table E5) achieved an AUC of 0.92 (95% confidence interval [CI], 0.83–1.00) in the cohort 1 validation set (Figure 3C) and was selected for further confirmation. This was performed in cohort 2, which comprised an independent set of 53 patients ($n = 17$ melioidosis, $n = 35$ other infections) from the Ubon-Sepsis study. Characteristics of cohort 2 patients are summarized in Table E6. The diagnostic signature achieved an AUC of 0.87 (95% CI, 0.77–0.97) in identifying melioidosis cases in cohort 2 (Figure 3D). These results indicate that measuring a limited number of circulating metabolites during initial presentation has significant potential for early diagnosis of melioidosis.

### Differentially Abundant Metabolites and Pathways Distinguish Fatal Melioidosis

Why melioidosis is associated with high mortality is not completely understood. To gain insights into the underlying pathophysiology preceding death, the metabolic features and biological pathways in plasma associated with death were analyzed. When melioidosis nonsurvivors were compared with survivors, 341 metabolites were differentially altered after adjusting for age, sex, BMI, and chronic kidney disease (Figure 4A and Table E3E). Lactate, a well-established marker for sepsis, was significantly elevated in the nonsurvivors (Figure 4B). Sixty-one out of 67 pathways were significantly altered in nonsurvivors from melioidosis compared with survivors (Figure 4C and Table E7). All 13 significant pathways within the Amino Acid superpathway were enriched in melioidosis nonsurvivors, such as Leucine, Isoleucine, and Valine Metabolism; Tryptophan Metabolism; Polyamine Metabolism; Glutamate Metabolism; Tyrosine Metabolism; and Urea cycle, Arginine and Proline Metabolism pathways (Figure 4C and Table E7). For example, 2-hydroxy-3-methylvalerate in the Leucine, Isoleucine, and Valine Metabolism pathway; urea in the Urea cycle, Arginine and Proline Metabolism pathway; and N(′1)-acetylspermidine in the Polyamine Metabolism pathway were all more abundant among the fatal melioidosis cases (Figure 4B). The decreased levels of tryptophan and increased levels of kynurenine among nonsurvivors (Figure 4B) suggest activation of the Tryptophan Metabolism pathway. After calculating the kynurenine-to-tryptophan ratio, we found this ratio was significantly elevated among fatal melioidosis cases (Figure E3B). Lipid metabolism was significantly altered in melioidosis nonsurvivors (Figure 4A), including the strikingly less abundant lysophospholipids and the more abundant medium-chain acylcarnitines (such as hexanoylcarnitine [C6] in Figure 4B) (Figure 4C and Tables E3E and E7). Several sphingomyelins were also associated with melioidosis mortality; levels of sphingomyelin (d18:1/20:0, d16:1/22:0), sphingomyelin (d18:1/25:0, d19:0/24:1, d20:1/23:0, d19:1/24:0), sphingomyelin (d18:1/20:1, d18:2/20:0), stearoyl sphingomyelin (d18:1/18:0), and sphingomyelin (d18:1/21:0, d17:1/22:0, d16:1/23:0) were all reduced in patients with fatal melioidosis (Table E3E). Of the 341 differentially expressed metabolites in nonsurvivors of melioidosis, 50 overlapped with those associated with death from other infectious etiologies (Table E3F), indicating that many of the metabolomic signals associated with fatal melioidosis may reflect responses specific to *B. pseudomallei* infection.

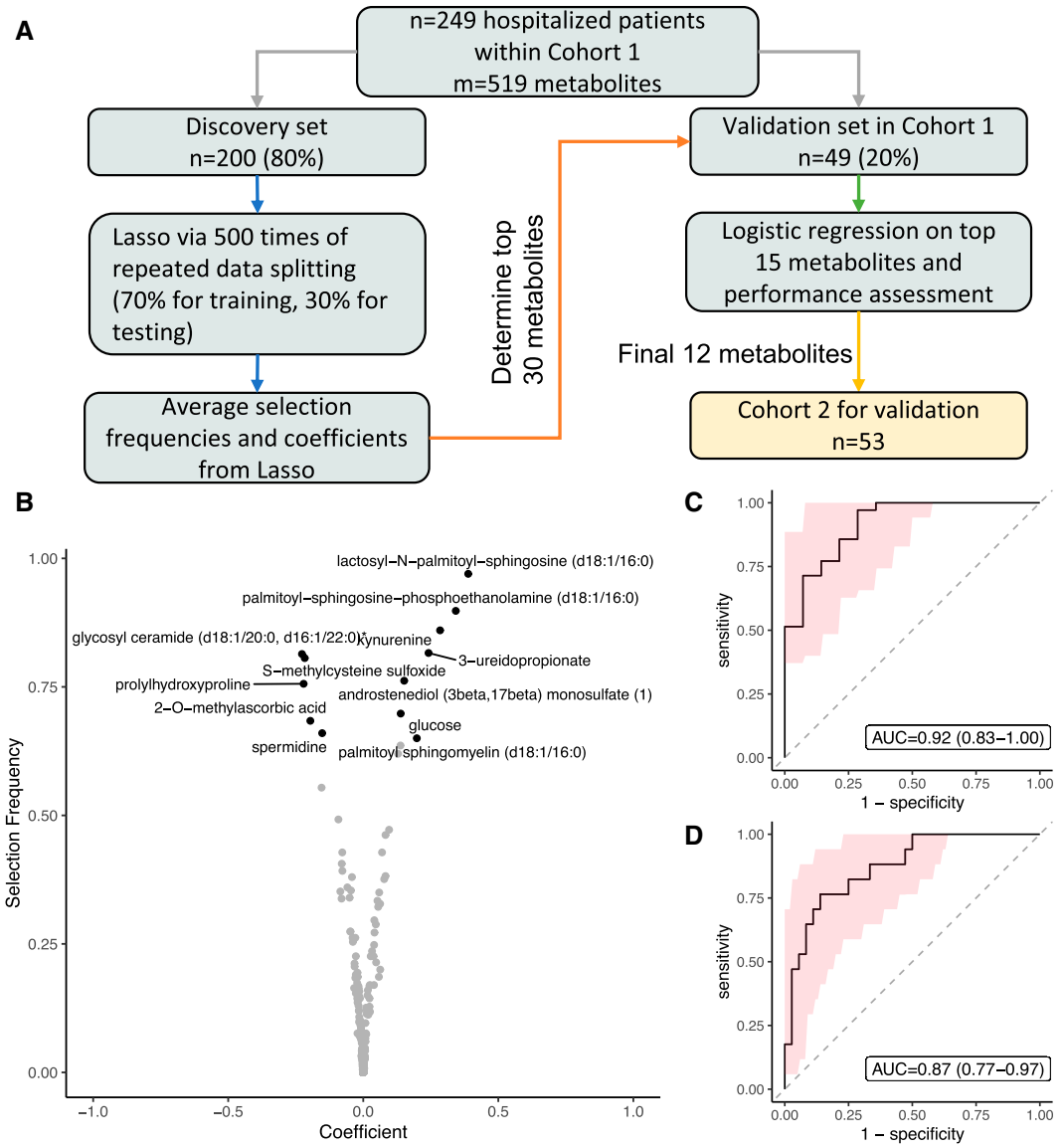


**Figure 3.** (*A*) Flow chart indicating construction and validation of the 12-metabolite signature for melioidosis diagnosis. (*B*) Average selection frequency (*y*-axis) and coefficient estimates (*x*-axis) in the repeated sample splitting with Lasso for identifying melioidosis cases. Receiver operating characteristic curves for identifying melioidosis cases in: (*C*) the validation set within cohort 1 ($n = 49$), and (*D*) the cohort 2 validation set ($n = 53$), using a 12-metabolite signature comprising the labeled metabolites in *B*. The AUC (95% confidence interval) was computed for each curve. AUC = area under the receiver operating characteristic curve.

**Metabolomic Biomarkers Predict Mortality in Patients with Melioidosis**

Given the high mortality associated with melioidosis, early identification of patients at increased risk for death is urgently needed. To identify a prognostic metabolomic signature, the patients with melioidosis from cohort 1 were split into discovery ($n = 140$) and validation ($n = 35$) sets and analyzed similarly to the diagnostic biomarker approach. Repeated data splitting with Lasso based on 519 metabolites in the discovery group generated a list of top metabolites ranked by selection frequency (Figure 4D). The top 15 metabolites were sequentially examined in the cohort 1 validation set ($n = 35$), which resulted in a selection of eight metabolites based on AUCs (Figure E4B): malate, glutamate, lactate, N(′1)-acetylspermidine, cis-4-decenoate (10:1n6), phosphoethanolamine, 1-methyladenosine, and ximenoylcarnitine (C26:1). This eight-metabolite panel achieved an AUC of 0.91 (95% CI, 0.82–1.00) in the cohort 1 validation set (Figure 4E). Because of the small sample size of patients with melioidosis in cohort 2 ($n = 17$), we evaluated the utility of these eight metabolites for predicting mortality in cohort 2 using hierarchical clustering and found reasonable performance in segregating survivors from nonsurvivors of melioidosis (Figure 4F).

## Discussion

Melioidosis is an emerging infection caused by the gram-negative bacterium *B. pseudomallei* that commonly presents as severe sepsis and is often lethal in endemic tropical regions despite appropriate antimicrobial treatment (20). As with many

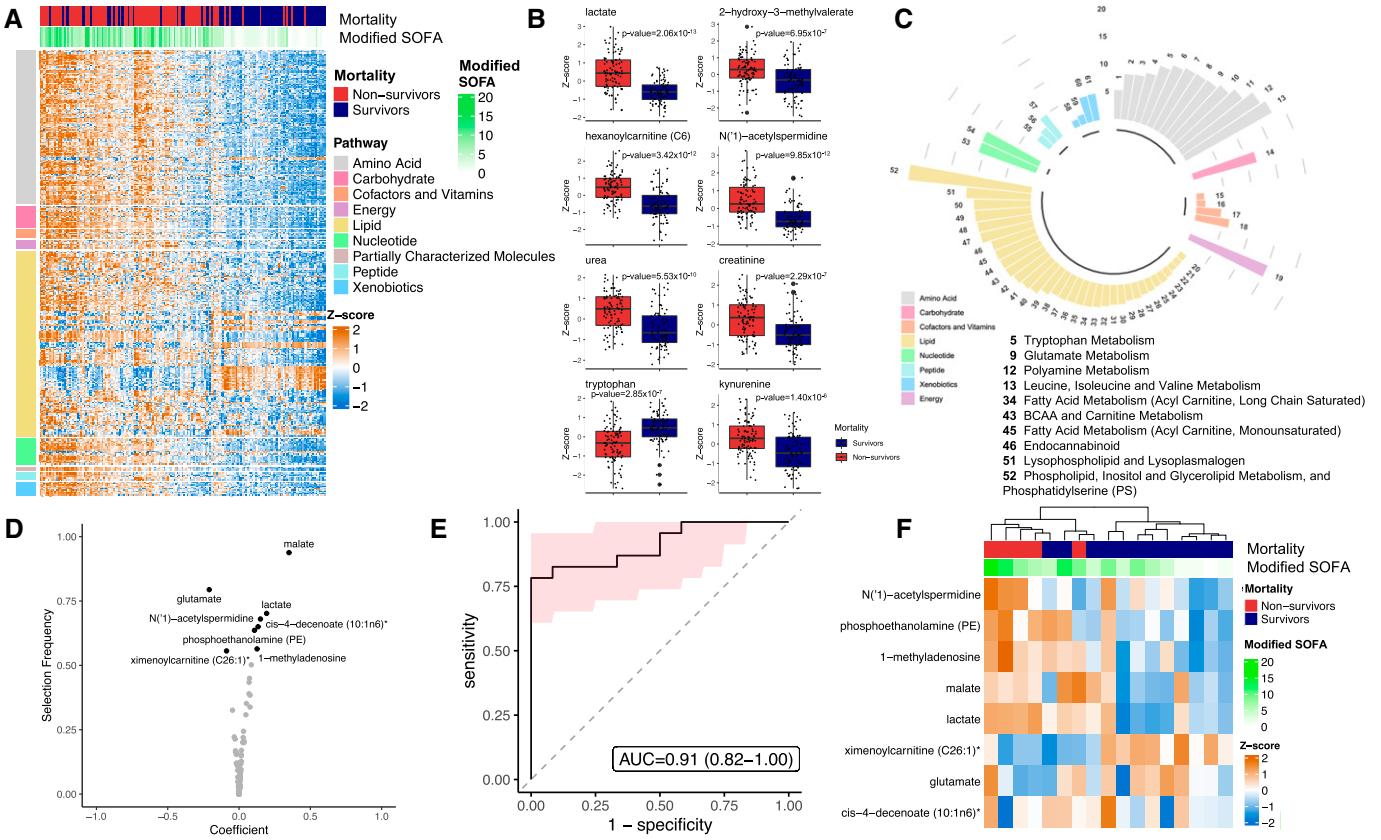


**Figure 4.** (*A*) Heatmap of 341 significantly differentially abundant metabolites, adjusted for age, sex, body mass index (BMI), and chronic kidney disease, comparing nonsurvivors versus survivors among patients with melioidosis. (*B*) Boxplots of eight representative metabolites from various pathways comparing melioidosis nonsurvivors to survivors. *P* values shown were calculated using Welch's *t* test. (*C*) Barplot of 61 significant pathways, obtained from the global test, comparing melioidosis nonsurvivors to survivors adjusting for age, sex, BMI, and chronic kidney disease; height of the bars represents negative $\log_{10}$ of Holm's procedure adjusted *P* values. (*D*) Average selection frequency (*y*-axis) and coefficient estimates (*x*-axis) in the repeated sample splitting with Lasso for identifying fatal melioidosis cases. (*E*) Receiver operating characteristic curve for identifying fatal melioidosis cases in the validation set within cohort 1 ($n = 35$), using the eight-metabolite signature labeled in *D*. The AUC (95% confidence interval) was computed for each curve. (*F*) Cluster analysis of the patients with melioidosis in the cohort 2 validation set ($n = 17$) using the eight-metabolite signature. AUC = area under the receiver operating characteristic curve; BCAA = branched-chain amino acids; SOFA = Sequential Organ Failure Assessment.

causes of sepsis, there are no effective vaccines or targeted immunotherapies. Given its health burden, developing a deeper understanding of the pathophysiology of melioidosis is essential. We leveraged a prospectively collected cohort of patients hospitalized with infection in rural Thailand to demonstrate the potential of applying agnostic "omics" analyses to the study of high-priority pathogens that cause severe infection and sepsis in low-resource settings. These results represent an important advance in efforts to reduce the global burden of severe infection and sepsis.

Complementary to existing literature on sepsis, our results indicate that hospitalized patients with infection have profound metabolomic changes compared with uninfected control subjects, confirming a vastly altered biological state (online supplement). Although severe infection resulting in hospitalization induces many common metabolic signals regardless of the etiologic pathogen, our observation suggests a unique metabo-inflammatory state in melioidosis, which can be probed to gain new insights into the pathophysiology of this disease and its adverse outcomes, including death.

Lipid metabolites in particular seem to be highly abundant in patients with melioidosis relative to patients with other infections, including important ceramides, sphingomyelins, PEs, lactosylceramides, and steroid hormones. Ceramides are released from sphingomyelins by sphingomyelinase in response to multiple stimuli, including stress and inflammation, and generated *de novo* or by salvage of sphingosine (21, 22). Ceramides appear to modulate cell membrane function and are implicated in internalization of pathogens (23, 24). This is a potentially relevant pathway, given that *B. pseudomallei* is a facultatively intracellular pathogen. We also detected increased levels of palmitoyl sphingomyelin (d18:1/16:0) and sphingomyelin (d18:2/16:0, d18:1/16:1) among patients with melioidosis. Sphingomyelin (d18:2/16:0) was previously found to be a potential biomarker for diagnosis of melioidosis (25). Notably, *B. pseudomallei* secretes a sphingosine-1-phosphate lyase ortholog, and this has been identified as a virulence factor for the pathogen (26, 27). Elevated levels of ceramides and sphingomyelins persisted even after adjusting for modified SOFA

score, an indicator of severity of illness. Adenosine, a natural purine nucleoside, was the most significantly abundant metabolite in melioidosis versus other infections (both with and without modified SOFA score adjustment). Elevated adenosine levels may reflect immunoregulatory activities of regulatory T cells and can bind to adenosine receptors (e.g., the A2a receptors) that induce immunosuppressive activities (28, 29).

Tryptophan metabolism was the second most significant and the third largest among the identified significantly altered pathways when comparing the metabolome in patients with melioidosis relative to patients with other infections. Tryptophan is an essential amino acid that is usually incorporated into proteins and has other important metabolic functions, such as the synthesis of hormones (e.g., kynurenine and serotonin) and coenzymes nicotinamide adenine dinucleotide (30–32). Tryptophan catabolism along the kynurenine pathway results in reduction in serotonin production and increased oxidative stress and inflammation that is reflected by elevated levels of the kynurenine metabolites (32). The kynurenine pathway plays key roles in cellular energy generation and in regulating inflammatory and immune responses (33). Our finding of elevated kynurenine levels in melioidosis suggests increased tryptophan degradation, a metabolic state linked to disease severity and case fatality in bacteremia (34) as well as modulation of T cell function (35). We also found a significantly increased kynurenine-to-tryptophan ratio in patients with melioidosis compared with patients with other infections, and in fatal melioidosis cases compared with nonfatal cases. This indicates greater activity of indoleamine 2,3-dioxygenase, a rate-limiting enzyme for tryptophan catabolism that is associated with disease severity and mortality in bacteremia (34, 36) and may play an important role in immunoregulatory mechanisms by inhibiting T cell proliferation (37).

This work is the first large-scale evaluation of metabolomic profiles associated with fatal melioidosis. We observed significant increases in free fatty acids and acylcarnitines in nonsurvivors compared with survivors among patients with melioidosis. Because free fatty acids and acylcarnitines play essential roles in energy metabolism and increase during human starvation (38), our findings indicate that nonsurvivors of melioidosis may be experiencing a more severe fasting metabolic state. Although the role of fasting metabolism and ketosis is complex during infection (39), elevated levels of circulatory acylcarnitines have been associated with poor outcomes in sepsis and overall mortality (40, 41). Specifically, increased levels of short- and medium-chain acylcarnitines in plasma have been associated with renal dysfunction, thrombocytopenia, and hyperlactatemia among critically ill patients (40), which is consistent with the observed increased levels of urea, creatinine, and lactate—markers of organ dysfunction—among nonsurvivors in our melioidosis cohort.

In contrast, we observed that increased abundance of several sphingomyelins carrying very long–chain fatty acids (fatty acids of 20 carbons or more) was associated with lower melioidosis mortality. Interestingly, we have previously reported that elevated plasma levels of sphingomyelins carrying very long–chain saturated fatty acids sphingomyelin (d18:1/20:0), sphingomyelin (d18:1/22:0), and sphingomyelin (d18:1/24:0) are associated with lower all-cause mortality in a large prospective cohort of older adults (42). Despite differences in study populations, these overlapping results suggest common underlying pathways and metabolites are linked to reduced risk of death.

In addition to providing new insights into the biological underpinnings of melioidosis, metabolomic signals were leveraged to derive and validate a 12-metabolite signature that showed promise as a clinical tool for early identification of melioidosis and deserves further evaluation. Of note, the most frequently selected elevated metabolite that was included in our diagnostic signature was lactosyl-N-palmitoyl-sphingosine (d18:1/16:0), a lactosylceramide that plays a critical role in the host response to bacterial infection as a pattern recognition receptor (43). This suggests biological plausibility of metabolites chosen for this signature. If confirmed in independent cohorts, this 12-metabolite blood-based diagnostic has the potential to be clinically valuable for early identification of melioidosis. This is because the current mainstay of melioidosis diagnosis is bacterial culture, which takes several days to yield results. In contrast, targeted measurement of a limited panel of plasma metabolites within the clinical laboratory setting may significantly expedite the diagnosis. Confidently establishing the etiology of infection early in the course of disease with plasma biomarkers allows the administration of appropriate antimicrobials—a crucial step when treating inherently antibiotic-resistant *B. pseudomallei*—while expediting triage and referral decisions and potentially improving outcomes.

We also assessed the performance of an eight-metabolite panel for predicting 28-day mortality in melioidosis that yielded a robust AUC of 0.91 in the validation subset of cohort 1 and demonstrated promising potential in segregating fatal from nonfatal melioidosis in the smaller cohort 2. Several of these prognostic metabolites have biological relevance in pathways leading to poor clinical outcomes. Higher levels of malate and lactate in fatal melioidosis cases reflect disturbance in energy metabolism under stressful conditions, especially in the tricarboxylic acid cycle and glycolysis. Lactate is a well-known marker of septic shock (44, 45) and, together with malate, has been linked to death from sepsis (7). Our prognostic signature indicates that lower glutamate levels are associated with fatal melioidosis, a finding that is consistent with previous reports of reduced glutamate levels in nonsurvivors of severe sepsis and its potential utility as an early biomarker for death in septic shock (46). Although promising, this prognostic signature requires further investigation in an independent cohort of patients with melioidosis and comparison to other predictive biomarkers and clinical tools (9, 15, 47–49).

To the best of our knowledge, this is the largest study of metabolomics in melioidosis to date on a deeply phenotyped cohort and one of the few investigations to apply metabolomics to identify the causative agent of severe infection in a low-resource setting. The prospective nature of the severe infection cohort, the systematic approach to hospitalized patient enrollment independent of cause of infection, and the early time point at which plasma was collected from hospitalized patients are strengths of this study. In addition, we used a large-scale and validated ultrahigh-performance liquid chromatography–tandem mass spectroscopy metabolomics platform to assess the plasma metabolome. However, there are also important limitations. These include the recruitment of hospitalized patients from a single referral center in northeastern Thailand, although these individuals were referred from more than 60 hospitals across the region. Causes of

infection were not known for some of the patients (i.e., the culture-negative group). Severity of illness was determined using a modified SOFA score that may not have completely captured the breadth of organ dysfunction experienced by patients. Although we analyzed additional patients from the parent cohort for confirmation of our diagnostic and prognostic signatures, validation in a separate cohort is needed to ensure generalizability of the findings. However, at present there are few prospective cohorts of patients with sepsis in melioidosis-endemic regions.

In conclusion, this investigation furnishes important and novel insights into the pathophysiology of melioidosis and proposes promising metabolite biomarker panels for diagnosis and prediction of this emerging global threat. ■

**Author disclosures** are available with the text of this article at www.atsjournals.org.

**Acknowledgment:** The authors thank Lara Lovelace-Macon for assistance with sample management.

## References

1. Rudd KE, Johnson SC, Agesa KM, Shackelford KA, Tsoi D, Kievlan DR, *et al.* Global, regional, and national sepsis incidence and mortality, 1990-2017: analysis for the Global Burden of Disease Study. *Lancet* 2020; 395:200–211.
2. Rudd KE, Kissoon N, Limmathurotsakul D, Bory S, Mutahunga B, Seymour CW, *et al.* The global burden of sepsis: barriers and potential solutions. *Crit Care* 2018;22:232.
3. Wiersinga WJ, Virk HS, Torres AG, Currie BJ, Peacock SJ, Dance DAB, *et al.* Melioidosis. *Nat Rev Dis Primers* 2018;4:17107.
4. Centers for Disease Control and Prevention. Bacteria that causes rare disease melioidosis discovered in U.S. environmental samples. 2022 [accessed 2023 Jun 26]. Available from: https://www.cdc.gov/media/releases/2022/p0727-Melioidosis.html.
5. Diray-Arce J, Conti MG, Petrova B, Kanarek N, Angelidou A, Levy O. Integrative metabolomics to identify molecular signatures of responses to vaccines and infections. *Metabolites* 2020;10:492.
6. Eckerle M, Ambroggio L, Puskarich MA, Winston B, Jones AE, Standiford TJ, *et al.* Metabolomics as a driver in advancing precision medicine in sepsis. *Pharmacotherapy* 2017;37:1023–1032.
7. Langley RJ, Tsalik EL, van Velkinburgh JC, Glickman SW, Rice BJ, Wang C, *et al.* An integrated clinico-metabolomic model improves prediction of death in sepsis. *Sci Transl Med* 2013;5:195ra95.
8. Seymour CW, Yende S, Scott MJ, Pribis J, Mohney RP, Bell LN, *et al.* Metabolomics in pneumonia and sepsis: an analysis of the GenIMS cohort study. *Intensive Care Med* 2013;39:1423–1434.
9. Wright SW, Kaewarpai T, Lovelace-Macon L, Ducken D, Hantrakun V, Rudd KE, *et al.* A 2-biomarker model augments clinical prediction of mortality in melioidosis. *Clin Infect Dis* 2021;72:821–828.
10. Hantrakun V, Somayaji R, Teparrukkul P, Boonsri C, Rudd K, Day NPJ, *et al.* Clinical epidemiology and outcomes of community acquired infection and sepsis among hospitalized patients in a resource limited setting in Northeast Thailand: a prospective observational study (Ubon-sepsis). *PLoS One* 2018;13:e0204509.
11. Teparrukkul P, Hantrakun V, Day NPJ, West TE, Limmathurotsakul D. Management and outcomes of severe dengue patients presenting with sepsis in a tropical country. *PLoS One* 2017;12:e0176233.
12. Rudd KE, Hantrakun V, Somayaji R, Booraphun S, Boonsri C, Fitzpatrick AL, *et al.* Early management of sepsis in medical patients in rural Thailand: a single-center prospective observational study. *J Intensive Care* 2019;7:55.
13. Booraphun S, Hantrakun V, Siriboon S, Boonsri C, Poomthong P, Singkaew B-O, *et al.* Effectiveness of a sepsis programme in a resource-limited setting: a retrospective analysis of data of a prospective observational study (Ubon-sepsis). *BMJ Open* 2021;11:e041022.
14. Somayaji R, Hantrakun V, Teparrukkul P, Wongsuvan G, Rudd KE, Day NPJ, *et al.* Comparative clinical characteristics and outcomes of patients with community acquired bacteremia caused by *Escherichia coli*, *Burkholderia pseudomallei* and *Staphylococcus aureus*: a prospective observational study (Ubon-sepsis). *PLoS Negl Trop Dis* 2021;15:e0009704.
15. Wright SW, Lovelace-Macon L, Hantrakun V, Rudd KE, Teparrukkul P, Kosamo S, *et al.* sTREM-1 predicts mortality in hospitalized patients with infection in a tropical, middle-income country. *BMC Med* 2020;18:159.
16. Teparrukkul P, Hantrakun V, Imwong M, Teerawattanasook N, Wongsuvan G, Day NPJ, *et al.* Utility of qSOFA and modified SOFA in severe malaria presenting as sepsis. *PLoS One* 2019;14:e0223457.
17. McInnes L, Healy J, Saul N, Großberger L. UMAP: uniform manifold approximation and projection. *J Open Source Softw* 2018;3:861.
18. Goeman JJ, van de Geer SA, de Kort F, van Houwelingen HC. A global test for groups of genes: testing association with a clinical outcome. *Bioinformatics* 2004;20:93–99.
19. Friedman J, Hastie T, Tibshirani R. Regularization paths for generalized linear models via coordinate descent. *J Stat Softw* 2010;33:1–22.
20. Chantratita N, Phunpang R, Yarasai A, Dulsuk A, Yimthin T, Onofrey LA, *et al.* Characteristics and one year outcomes of melioidosis patients in Northeastern Thailand: a prospective, multicenter cohort study. *Lancet Reg Health Southeast Asia* 2023;9:100118.
21. Maceyka M, Spiegel S. Sphingolipid metabolites in inflammatory disease. *Nature* 2014;510:58–67.
22. Stith JL, Velazquez FN, Obeid LM. Advances in determining signaling mechanisms of ceramide and role in disease. *J Lipid Res* 2019;60: 913–918.
23. Grassmé H, Becker KA, Zhang Y, Gulbins E. Ceramide in bacterial infections and cystic fibrosis. *Biol Chem* 2008;389:1371–1379.
24. Grassmé H, Becker KA. Bacterial infections and ceramide. *Handb Exp Pharmacol* 2013;216:305–320.
25. Lau SKP, Lee K-C, Lo GCS, Ding VSY, Chow W-N, Ke TYH, *et al.* Metabolomic profiling of plasma from melioidosis patients using UHPLC-QTOF MS reveals novel biomarkers for diagnosis. *Int J Mol Sci* 2016;17:307.
26. Custódio R, McLean CJ, Scott AE, Lowther J, Kennedy A, Clarke DJ, *et al.* Characterization of secreted sphingosine-1-phosphate lyases required for virulence and intracellular survival of *Burkholderia pseudomallei*. *Mol Microbiol* 2016;102:1004–1019.
27. McLean CJ, Marles-Wright J, Custodio R, Lowther J, Kennedy AJ, Pollock J, *et al.* Characterization of homologous sphingosine-1-phosphate lyase isoforms in the bacterial pathogen *Burkholderia pseudomallei*. *J Lipid Res* 2017;58:137–150.
28. Ohta A, Sitkovsky M. Extracellular adenosine-mediated modulation of regulatory T cells. *Front Immunol* 2014;5:304.
29. Zhang T, Yu-Jing L, Ma T. The immunomodulatory function of adenosine in sepsis. *Front Immunol* 2022;13:936547.
30. Rodriguez Cetina Biefer H, Vasudevan A, Elkhal A. Aspects of tryptophan and nicotinamide adenine dinucleotide in immunity: a new twist in an old tale. *Int J Tryptophan Res* 2017;10:1178646917713491.
31. DiNatale BC, Murray IA, Schroeder JC, Flaveny CA, Lahoti TS, Laurenzana EM, *et al.* Kynurenic acid is a potent endogenous aryl hydrocarbon receptor ligand that synergistically induces interleukin-6 in the presence of inflammatory signaling. *Toxicol Sci* 2010;115:89–97.
32. Karu N, McKercher C, Nichols DS, Davies N, Shellie RA, Hilder EF, *et al.* Tryptophan metabolism, its relation to inflammation and stress markers and association with psychological and cognitive functioning: Tasmanian Chronic Kidney Disease pilot study. *BMC Nephrol* 2016; 17:171.
33. Zeden JP, Fusch G, Holtfreter B, Schefold JC, Reinke P, Domanska G, *et al.* Excessive tryptophan catabolism along the kynurenine pathway precedes ongoing sepsis in critically ill patients. *Anaesth Intensive Care* 2010;38:307–316.

34. Huttunen R, Syrjänen J, Aittoniemi J, Oja SS, Raitala A, Laine J, *et al.* High activity of indoleamine 2,3 dioxygenase enzyme predicts disease severity and case fatality in bacteremic patients. *Shock* 2010;33: 149–154.
35. Stone TW, Williams RO. Modulation of T cells by tryptophan metabolites in the kynurenine pathway. *Trends Pharmacol Sci* 2023;44: 442–456.
36. Tattevin P, Monnier D, Tribut O, Dulong J, Bescher N, Mourcin F, *et al.* Enhanced indoleamine 2,3-dioxygenase activity in patients with severe sepsis and septic shock. *J Infect Dis* 2010;201:956–966.
37. Hwu P, Du MX, Lapointe R, Do M, Taylor MW, Young HA. Indoleamine 2,3-dioxygenase production by human dendritic cells results in the inhibition of T cell proliferation. *J Immunol* 2000;164:3596–3599.
38. Steinhauser ML, Olenchock BA, O'Keefe J, Lun M, Pierce KA, Lee H, *et al.* The circulating metabolome of human starvation. *JCI Insight* 2018;3:e121434.
39. Wang A, Huen SC, Luan HH, Yu S, Zhang C, Gallezot J-D, *et al.* Opposing effects of fasting metabolism on tissue tolerance in bacterial and viral inflammation. *Cell* 2016;166:1512–1525.e12.
40. Chung K-P, Chen G-Y, Chuang T-Y, Huang Y-T, Chang H-T, Chen Y-F, *et al.* Increased plasma acetylcarnitine in sepsis is associated with multiple organ dysfunction and mortality: a multicenter cohort study. *Crit Care Med* 2019;47:210–218.
41. Ferrario M, Cambiaghi A, Brunelli L, Giordano S, Caironi P, Guatteri L, *et al.* Mortality prediction in patients with severe septic shock: a pilot study using a target metabolomics approach. *Sci Rep* 2016;6:20391.
42. Fretts AM, Jensen PN, Hoofnagle AN, McKnight B, Sitlani CM, Siscovick DS, *et al.* Circulating ceramides and sphingomyelins and risk of mortality: the Cardiovascular Health Study. *Clin Chem* 2021;67: 1650–1659.
43. Wang X, Nijman R, Camuzeaux S, Sands C, Jackson H, Kaforou M, *et al.*; EUCLIDS consortium. Plasma lipid profiles discriminate bacterial from viral infection in febrile children. *Sci Rep* 2019;9:17714.
44. Garcia-Alvarez M, Marik P, Bellomo R. Sepsis-associated hyperlactatemia. *Crit Care* 2014;18:503.
45. Han X, Edelson DP, Snyder A, Pettit N, Sokol S, Barc C, *et al.* Implications of Centers for Medicare & Medicaid Services Severe Sepsis and Septic Shock Early Management Bundle and initial lactate measurement on the management of sepsis. *Chest* 2018;154:302–308.
46. Poeze M, Luiking YC, Breedveld P, Manders S, Deutz NEP. Decreased plasma glutamate in early phases of septic shock with acute liver dysfunction is an independent predictor of survival. *Clin Nutr* 2008;27: 523–530.
47. Kaewarpai T, Wright SW, Yimthin T, Phunpang R, Dulsuk A, Lovelace-Macon L, *et al.* IL-1R2-based biomarker models predict melioidosis mortality independent of clinical data. *Front Med (Lausanne)* 2023;10: 1211265.
48. Wright SW, Hantrakun V, Rudd KE, Lau C-Y, Lie KC, Chau NVV, *et al.* Enhanced bedside mortality prediction combining point-of-care lactate and the quick Sequential Organ Failure Assessment (qSOFA) score in patients hospitalised with suspected infection in southeast Asia: a cohort study. *Lancet Glob Health* 2022;10:e1281–e1288.
49. Kaewarpai T, Ekchariyawat P, Phunpang R, Wright SW, Dulsuk A, Moonmueangsan B, *et al.* Longitudinal profiling of plasma cytokines in melioidosis and their association with mortality: a prospective cohort study. *Clin Microbiol Infect* 2020;26:783.e1–783.e8.